

# Photovoltaic Properties of n-(CdO)<sub>1-x</sub>(SnO<sub>2</sub>)<sub>x</sub>/p-Si Heterojunction Prepared by Pulsed Laser Deposition

Mohammed A. Abdul Majeed<sup>1,\*</sup>, Nahida B. Hasan<sup>1</sup>, Ghusson H. Mohammed<sup>2</sup>

<sup>1</sup>Department of Physics, Collage of Science, University of Babylon, Babylon, Iraq

<sup>2</sup>Department of Physics, Collage of Science, University of Baghdad, Baghdad, Iraq

**Abstract** CdO heterojunction can be synthesized and formed into an ultraviolet (UV) photodetector at different concentration of SnO<sub>2</sub> (x = (0.0, 0.05, 0.1, 0.15 and 0.2)) Wt. % onto a silicon wafer substrate by pulsed laser deposition technique (PLD) using Nd-YAG laser with  $\lambda=1064\text{nm}$ , energy=600mJ and number of shots=500. The spectral response of n-(CdO)<sub>1-x</sub>(SnO<sub>2</sub>)<sub>x</sub>/p-Si was studied. The influence of SnO<sub>2</sub> content on the photovoltaic properties of CdO heterojunctions is studied. The values of responsivity, specific detectivity and quantum efficiency decrease and shift to short wavelength with increase of concentration SnO<sub>2</sub>. Good photoresponse to UV light has been demonstrated for CdO doped with SnO<sub>2</sub> heterojunction photodetectors when increases SnO<sub>2</sub> was investigated. A high broad peaks are observed around  $\lambda=550\text{nm}$  for pure CdO and shift to  $\lambda=300\text{nm}$  when doping with 0.25 wt SnO<sub>2</sub>.

**Keywords** Heterojunction, CdO films, SnO<sub>2</sub> films, Pulsed laser deposition, Photovoltaic properties

## 1. Introduction

Cadmium Oxide CdO is unique combination of various thin film properties which were represented by high electrical conductivity, high carrier concentrations and high transparency in the visible range of the electromagnetic spectrum, made it suitable for a wide range of applications in different fields [7, 6]. The applications of CdO thin films are in photovoltaic solar cells for front contacts window layer, or as heterostructure such as CdO/CdTe or CdO/Cu<sub>2</sub>O solar cells [1, 8, 9], Photoelectrochemical devices [3], Phototransistors [3, 5], photodiodes [2, 4], Liquid crystal displays [5, 4], - Antireflection coatings [3], IR detectors [5] and Gas sensors [1-4].

- Transparent electrodes was used as transparent anodes for organic light emitting (OLEDs) as a practical new display technology [1, 3]. It has been used as heat mirrors, due to its high reflectance in the infrared region together with transparency in the visible region [4]. Stannic Oxide SnO<sub>2</sub> In 1942 Masters [10] succeeded in preparing conductive transparent tin oxide, for the first time. A substance with white color has a molecular weight of (150. 69 g/mol). Its density (6.95 g/cm<sup>3</sup>), its melting point (1630°C) and its boiling point (1900°C) [11]. Stannic oxide is an n- type semiconducting material with a direct band gap of about 4.0 eV and an indirect band gap of about 2.6 eV [12]. The

electron concentration in the conduction band arises primarily from the lack of stoichiometry produced by oxygen deficiency. The property of SnO<sub>2</sub> makes the material useful for many applications. There for increasing attention is begin paid to study this oxide especially on the method of operation, and its electrical and optical properties. SnO<sub>2</sub> thin films have been fabricated using different techniques including pulse laser deposition, electron beam evaporation [13], chemical vapor deposition [14], RF sputtering [15], evaporation and chemical spray pyrolysis [16]. SnO<sub>2</sub> as transparent conducting oxide is used extensively for a variety of applications such as transparent electrodes in solar cells, architectural windows and flat panel displays [17]. Recently SnO<sub>2</sub> has been integrated into micro chemical silicon devices as a sensing element of micro sensor.

## 2. Experimental

### 2.1. Preparation Pellets

High purity powders (99.999%) of CdO and SnO<sub>2</sub> supplied from Fluka were used to form the target as a disk of 2.5cm diameter and 0.4 cm thickness by pressing it under 4 ton force. The pellets which containing the elements were heated to 873K for 3 hours then cooled to room temperature. The temperature of the furnace was raised at a rate of 10°C/min. The amount of elements content of pellets was evaluated by using the following equation.

$$W_{(\text{CdO})_{1-x}(\text{SnO}_2)_x} = W_{\text{CdO}} \times (1-x) + W_{\text{SnO}_2} \times (x) \quad (1)$$

Where:  $W_{\text{CdO}}=128.411$  ( atomicweight for CdO),

\* Corresponding author:

moh950611@gmail.com (Mohammed A. Abdul Majeed)

Published online at <http://journal.sapub.org/ajcmp>

Copyright © 2015 Scientific & Academic Publishing. All Rights Reserved

$W_{\text{SnO}_2}=150.69$  (atomic weight for  $\text{SnO}_2$ ) and  $x=0, 0.05, 0.1, 0.15$  and  $0.2$  (concentration of  $\text{SnO}_2$ ).

## 2.2. Preparation of Porous Silicon Layer by Photochemical Etching

The p-type Si wafer of (0.05  $\Omega \cdot \text{cm}$ ) resistivity was used as a starting substrate in the photochemical etching. The samples of ( $1.5 \times 1.5 \text{ cm}^2$ ) dimensions were cut from the wafer and rinsed with acetone and methanol to remove dirt. The photochemical etching is electrodeless process since there is no applied bias voltage during the etching, this process is carried out by using ordinary light source. The setup consists of a Quartz Tungsten Halogen lamps (250W) integrated with dichroic ellipsoidal mirror supplied from Philips Company, focusing lens and the diluted etching acid in container. In order to remove the native oxide layer on the samples, they were etched in diluted (10%) HF acid. After cleaning the samples they were immersed in HF acid of 50% concentration and ethanol 50% in a container.

The light source was vertically mounted by a holder above the sample, aligned and focused by Quartz lens of (3.87cm) focal length to form a circular spot with a suitable power density. The lens was mounted on a driven holder for precise focusing adjustment. The distance from the lamp to the lens was about 30 cm and from the lens to the sample 14 cm. The PS was formed on the illuminated side of the sample. The photo etching irradiation times was chose to be about 10 minutes.

At the end of the photochemical etching process, the sample were rinsed with ethanol and stored in a glass containers filled with methanol to avoid the formation of oxide layer above the nanospikes thin film. The nanospikes silicon layers were used as a substrate for  $(\text{CdO})_{1-x}(\text{SnO}_2)_x$  the photoconductive detector elements.

## 2.3. Thin Film Preparation and Characterization

The  $(\text{CdO})_{1-x}(\text{SnO}_2)_x$  heterojunction were deposited porous silicon wafers of (100) orientation were used in this work heterojunction at room temperature by PLD technique using Nd:YAG with  $\lambda = 1064 \text{ nm}$  SHG Q-switching laser beam at 600 mJ, repetition frequency (6Hz) for 500 laser pulse is incident on the target surface making an angle of  $45^\circ$ . The under vacuum of ( $10^{-3} \text{ mbar}$ ) at room temperature. DC power supply (0-15V, 0-2 A), a variable resistance is used to limit the detector bias current. A PC-interfaced digital Multimeter and Laptop PC are used to register the output circuit current. The UV - Led is used as a UV source for illumination of the CdO:  $\text{SnO}_2$  photoconductive UV detector. The optical power of the UV Led is 2.5mW and the wavelength is about 385 nm.

# 3. Results and Discussion

## 3.1. Spectral Measurements for $(\text{CdO})_{1-x}(\text{SnO}_2)_x/\text{p-Si}$ Heterojunction

### 3.1.1. Spectral Responsivity ( $R_\lambda$ )

Spectral responsivity ( $R_\lambda$ ) is the most important parameter by which the range of heterojunction operation can be determined using equation [18].

$$R_\lambda = \frac{V}{P_{\text{in}}} \quad (\text{Volt / Watt}) \quad (2)$$

Figure (1) shows the variation of the spectral responsivity with the wavelength for  $(\text{CdO})_{1-x}(\text{SnO}_2)_x$  heterojunction at different concentration  $\text{SnO}_2$  ( $x=0, 0.05, 0.1, 0.15$  and  $0.2$ ). One can notice from the figure that two peaks is appear, the one peak donated for  $(\text{CdO})_{1-x}(\text{SnO}_2)_x$  in the visible range around (300-550)nm and another peak for p-Si around (750-800)nm That increasing of the  $(\text{CdO})_{1-x}(\text{SnO}_2)_x$  films concentration causes a decreasing in the spectral responsivity value for all wavelength range and shifts the peaks from visible region to UV region this means that by increasing  $\text{SnO}_2$  contents made the junctions work in the UV region detectors, this is because of increasing of the defect concentrations which act as recombination centers concentrated on the two sides of the interface. Therefore the photo-generated carriers recombine at a large rate. We can see from the same Table that the peaks of  $R_\lambda$  are shifted to shorter wavelength.

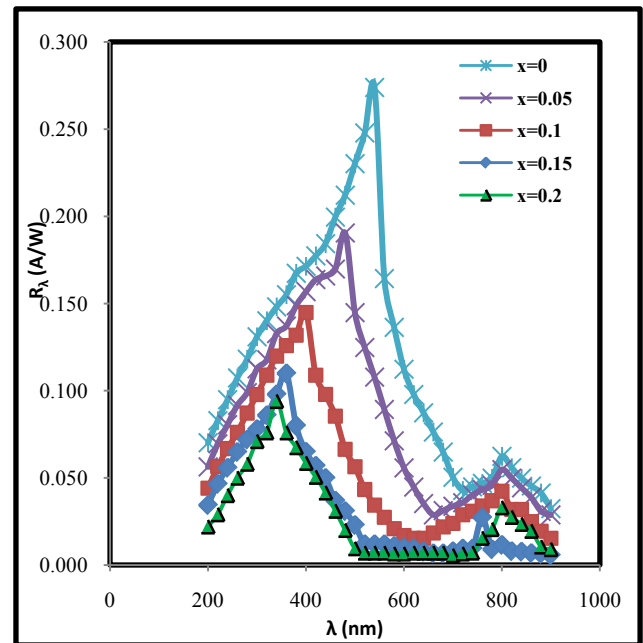


**Figure (1).** The variation of responsivite ( $R_\lambda$ ) with the wavelength for  $(\text{CdO})_{1-x}(\text{SnO}_2)_x/\text{p-Si}$  heterojunction with different concentration of  $\text{SnO}_2$

### 3.1.2. Noise Equivalent Power

The noise equivalent power (NEP) values were calculated using equation [18].

$$\text{NEP} = I_n / R_\lambda \quad (3)$$

Figure (2) and Table (1) Show the Noise Equivalent Power as a function of wavelength for  $(\text{CdO})_{1-x}(\text{SnO}_2)_x$  heterojunction at different concentration  $\text{SnO}_2$  ( $x=0, 0.05, 0.1, 0.15$  and  $0.2$ ). One can observe that the minimum NEP

occurs where  $R_{\lambda}$  has the maximum value this means that NEP has opposite behaviour than  $R_{\lambda}$  i.e increases with increasing of concentration.

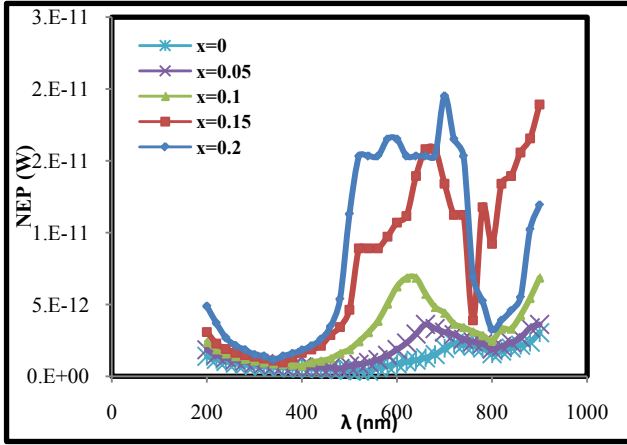


**Figure (2).** The variation of noise equivalent power with the wavelength for (CdO)<sub>1-x</sub>(SnO<sub>2</sub>)<sub>x</sub> heterojunction with different concentration of SnO<sub>2</sub>

3.1.3. The Specific Detectivity

The specific detectivity ( $D^*$ ) was calculated using equation [19].

$$D^* = D(A \cdot \square \cdot f)^{1/2} \tag{4}$$

The variation of  $D^*$  as a function of wavelength for (CdO)<sub>1-x</sub>(SnO<sub>2</sub>)<sub>x</sub> heterojunction at different concentrations SnO<sub>2</sub> (x=0, 0.05, 0.1, 0.15 and 0.2) is presented in Figure (3). It is obvious that the  $D^*$  value decreases with increasing of concentrations, as given in Table (1) this is the increase of the defects that lead to an increase of the recombination processes which affect the value of  $D^*$ .

3.1.4. Quantum Efficiency ( $\eta$  %)

The quantum efficiency ( $\eta$ ) is a very important parameter were calculated using equation [19].

$$\eta(\lambda) = R_{\lambda} \frac{h\nu}{q} = 1.24 \frac{R_{\lambda}}{\lambda} * 100\% \tag{5}$$

In the photovoltaic devices which is recognized by the optoelectronic effect. It represents the ratio between the numbers of generated electrons in the heterojunctions to the number of incident photons on the effective area of the heterojunctions. So, it related to the change of the spectral

responsivity as shown in Figure (4) and Table (1) due to the same reasons mentioned earlier for responsivity.

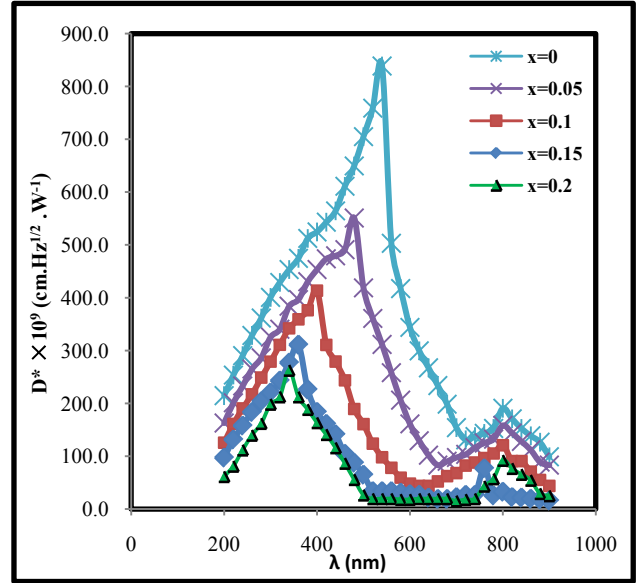


**Figure (3).** The variation of Specific Detectivity with the wavelength for (CdO)<sub>1-x</sub>(SnO<sub>2</sub>)<sub>x</sub>/p-Si heterojunction with different concentration of SnO<sub>2</sub>

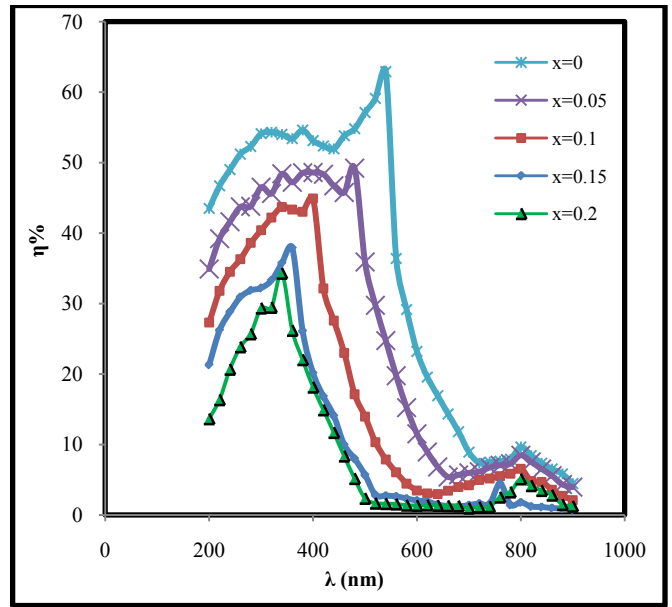


**Figure (4).** The variation of quantum efficiency with the wavelength for (CdO)<sub>1-x</sub>(SnO<sub>2</sub>)<sub>x</sub>/p-Si heterojunction with different concentration of SnO<sub>2</sub>

**Table (1).** The spectral parameters for (CdO)<sub>1-x</sub>(SnO<sub>2</sub>)<sub>x</sub>/p-Si photovoltaic heterojunction

x	$\lambda_{peak}$ (nm)	$R_{\lambda}$ (A/W)	$\eta$ %	NEP $\times 10^{-13}$ (Watt)	$D \times 10^{12}$ (cm.Hz <sup>1/2</sup> .W <sup>-1</sup> )	$D^* \times 10^{11}$ (cm.Hz <sup>1/2</sup> .W <sup>-1</sup> )
0	540	0.273	62.900	3.577	2.796	8.387
0.05	480	0.190	49.200	5.445	1.837	5.510
0.1	400	0.144	44.898	7.255	1.378	4.135
0.15	360	0.109	37.854	9.643	1.037	3.111
0.2	340	0.094	34.282	11.42	0.875	2.627

## 4. Conclusions

In conclusion, the CdO photovoltaic UV detector was developed using different concentrations of SnO<sub>2</sub> prepared by pulsed laser deposition technique. This device exhibits a prominent performance for UV light detection. The spectral response, specific detectivity and quantum efficiency of (CdO)<sub>1-x</sub>(SnO<sub>2</sub>)<sub>x</sub> heterojunction were investigated. It observed that these parameters decrease and shift to shorter wavelength with increasing of concentration of SnO<sub>2</sub>. Noise equivalent power increases with increasing of concentration of SnO<sub>2</sub>. The responsivity reached peak at  $\lambda = 550$  nm for pure CdO and this peak shift to 300 nm when SnO<sub>2</sub> content increases.

---

## REFERENCES

- [1] D. M. Galicia, R. C. Perez, O. J. Sandoval, S. J. S Sandoval and C. I. Z. Romero, *J. Thin Solid Film*, Vol. 371, pp. 105-108, (2000).
- [2] P. A. Radi, A. G. Brito, J. M. Madurro and N. O. Dantas, *Brazilian J. Physics*, Vol. 36, pp. 412-414, (2006).
- [3] R. S. Mane, H. M. Pathan, C. D. Lokhande and S. H. Han, *J. Solar Energy*, Vol. 80, pp. 185- 190, (2006).
- [4] P. Sinatirajah, *J. Applied Surface Science*, Vol. 254 (13), pp. 3813-3818, (2008).
- [5] C. H. Bhosale, A.V. Kambale, A. V. Kokate and K.Y. Rajpure, *J. Materials Science and Engineering*, Vol. B122, pp. 67-71, (2005).
- [6] X. Li, T. Gessert, C. Dehart, T. Barnes, J. Perkins and T. Coutts, proceeding of the NCPV Program Review Meeting, Colorado, (2001).
- [7] D. M. Ellis and S. J. Irvine, University of Wales, (2002).
- [8] K. Hame and S. E. San, *J. Solar Energy*, Vol. 77 (3), pp. 291-294, (2004).
- [9] S. Kose and F. Atay, *International J. Green Energy*, Vol. 1 (3), pp. 353-364, (2004).
- [10] J. C. Manificier, M. De-Murcia, J.P. Fillard, *Thin solid Films*, Vol.41, p. 127, (1977).
- [11] D. K. Lide, "Chemical Rubber Company Hand Book of chemistry and physics", CRC press, Boca Raton, Florida, USA, 77<sup>th</sup> ed., (1996).
- [12] J. E. Macintyner, Chapman and Hall, London, UK, Vol. 1-3, (1992).
- [13] W. I. Cho, H. Jang and S. R. Lee, *Script. Met.* Vol. 32, p. 815, (1995).
- [14] M.C. Giulio, G. Micocci, A. Serra, A. Tepore, R. Rella and P. Siciliano, *J. Sens. Actuators*, Vol. B 24 -25, P. 564, (1995).
- [15] M. C. Horrillo, P. Saotos and L. Manes, *J. Sens. Actuators*, Vol. B45, p. 193. (1997).
- [16] D. Liu, Q. Wang, H. I. M. Jang and H. Chen, *J. Mat. Res*, Vol. 10, p. 1516. (1995).
- [17] Y. Lin, W. Zhu, O. K. Tan and X. Tao, *J. Mat. Sci*, Vol.7, p. 279, (1996).
- [18] In-Soun Ryu and Kiyoshi Takashi, *Japanese J. Applied Physics*, Vol. 4, No.11, pp. 850-853, (1965).
- [19] R. Lever and E. Huminski, *J. Applied of Physics*, Vol. 37, No.8, pp. 3638-3639, (1966).